The 2010 IEEE/RSJ International Conference on
Intelligent Robots and Systems
October 18-22, 2010, Taipei, Taiwan

Energetic efficiency and stability of dynamic bipedal walking gaits with different step lengths

Yan Huang, Baojun Chen, Qining Wang, Kunlin Wei and Long Wang

Abstract— **This paper presents a seven-link dynamic walking model that is more close to human beings. We add hip actuation, upper body, flat feet and compliant ankle joints to the model. Walking sequence of the flat-foot walker has several sub-streams that form bipedal walking with dynamic series of phases, which is different with the motion of round-foot and point-foot models. We investigate the characteristics of three different walking gaits with different step lengths. Comparison of these walking gaits in walking velocity, efficiency and stability reveals the relation between step length and walking performance. Experimental results indicate that the gait which is more close to human normal walking achieves higher stability and energetic efficiency.**

I. Introduction

Human beings can achieve stable and efficient dynamic bipedal walking on various different terrains without much effort. Though people's usual gaits tend to be natural and simple, bipedal walking involves highly non-linear and multi-variable dynamics with discrete events and a varying configuration. To study human locomotion and construct bipedal robots, the trajectory-control approach has been proposed [1]. By controlling joint angles precisely, the humanoid robots can achieve static equilibrium postures at any time during motion. In such static walking gaits, the zero moment point (ZMP) has to be within the convex hull of the supporting area [2]. However, the corresponding energy consumption and requirements of actuators are relatively high.

Different from static walking, dynamic bipedal walkers may not reach static equilibrium at some time, but can realize stable cyclic walking. As an example, passive dynamic walking [3] has been presented as a possible explanation for the efficiency of the human gait, which showed that a mechanism with two legs can be constructed so as to descend a gentle slope with no actuation and no active control. Dynamic walking achieves high efficiency and shows a remarkable resemblance to the human gait.

Most studies of passive dynamic walking are based on the Simplest Walking Model [4] and extended work [5], which consist of two rigid massless legs connected by a frictionless hinge at the hip, with a large point mass at the hip and a small mass at each foot. In these models, passive walkers are often modeled with point feet or round feet which have clear disadvantages of being unable to achieve the start and stop of walking. However, only a few studies have been done on a flat foot shape in passive dynamic models [7], [8], [9]. These studies proposed that the flat foot with a geometric parameter (foot length) can introduce a toe-strike collision in addition to the heel-strike impulse and influence the passive dynamics of walking. In addition, compliant ankles have been added to passive dynamic walkers [11], [12], [13]. The mechanical energy stored in such elastic elements can be recovered as both kinetic and gravitational energy. It may improve the efficiency and adaptability of bipedal walking. Our recent study reported that dynamic walking models with flat feet and passive ankle springs can largely resemble real human walking [10]. However, in all these dynamic bipedal models, the walking phases are predetermined.

In this paper, we present a seven-link dynamic walking model that is more close to human beings. We add hip actuation, upper body, flat feet and compliant ankle joints to the model. Since flat-foot walker has multiple contact cases, the walking sequence is not predetermined, which is different from those of point-feet and round-feet walkers. Different combinations of contact conditions of the two leg generate different walking gaits. Thus we study walking characteristics of three typical dynamic bipedal walking gaits with flat feet, classified by step length. Comparison of walking performance of different gaits could help us better understand the locomotion of real human walking, which is the main motivation of this paper.

This paper is organized as follows. Section II presents the dynamic walking model in detail. Section III is devoted to describe the three typical walking gaits. Section IV gives the simulation results. We conclude in Section V.

II. Bipedal Walking Model

A. Flat-foot walker with compliant ankles

To study the motion characteristics of real human walking, we added flat feet and compliant ankle joints to the dynamic bipedal walking model. As shown in Fig. 1, the two-dimensional model consists of two rigid legs interconnected individually through a passive hinge with a rigid upper body (mass added stick) connected at the hip. Each leg includes thigh, shank and foot. The thigh and the shank are connected at the knee joint, while the foot is mounted on the ankle with a torsional spring.A point mass at hip represents the pelvis. The mass of each leg and foot is simplified as point mass added on the Center of Mass (CoM) of the shank, the thigh, and the foot, respectively.

Similar to [6], a kinematic coupling has been used in the model to keep the body midway between the two legs. In addition, our model added compliance in knee joints and

This work was supported by the 985 Project of Peking University (No. 3J0865600).

Y. Huang, B. Chen, Q. Wang and L. Wang are with the College of Engineering, Peking University, China. K. Wei is with the Department of Psychology, Peking University, China.

Email: Q. Wang (qiningwang@pku.edu.cn)

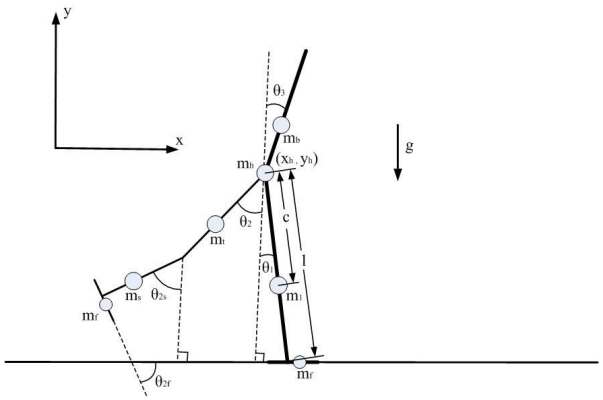

Fig. 1. Model of the dynamic walker with flat feet and compliant ankles.

ankle joints. Specifically, knee joints and ankle joints are modeled as passive joints that are constrained by torsional springs. To simplify the motion, we have some assumptions, including shanks and thighs suffering no flexible deformation, hip joint and knee joints with no damping or friction, the friction between walker and ground is enough, thus the flat feet do not deform or slip, and strike is modeled as an instantaneous, fully inelastic impact where no slip and no bounce occurs. The passive walker travels forward on level ground with hip actuation. We suppose that the x-axis is along the ground while the y-axis is vertical to the ground upwards. The configuration of the walker is defined by the coordinates of the point mass on hip joint and some angles (swing angles between vertical axis and each thigh and shank, angle between vertical axis and the upper body and the foot angles between horizontal coordinates and each foot) (See Fig. 1), which can be arranged in a generalized vector $q = (x_h, y_h, \theta_1, \theta_2, \theta_3, \theta_{2s}, \theta_{1f}, \theta_{2f})^T$. The positive directions of all the angles are counter-clockwise.

B. Dynamics of walking

The model can be defined by the euclidean coordinates x, which can be described by the x-coordinate and y-coordinate of the mass points and the corresponding angles (suppose leg 1 is the stance leg):

$$x = [x_h, y_h, x_{c1}, y_{c1}, \theta_1, x_{c2t}, y_{c2t}, \theta_2, x_{c3}, y_{c3}, \theta_3, x_{c2s}, y_{c2s}, \theta_{2s}, x_{c1f}, y_{c1f}, \theta_{1f}, x_{c2f}, y_{c2f}, \theta_{2f}]^T \quad (1)$$

The walker can also be described by the generalized coordinates q as mentioned before:

$$q = (x_h, y_h, \theta_1, \theta_2, \theta_3, \theta_{2s}, \theta_{1f}, \theta_{2f})^T \quad (2)$$

We defined matrix T as follows:

$$T = dq/dx \quad (3)$$

Thus T transfers the velocities of the euclidean coordinates $\dot{x}$ into the independent generalized coordinates $\dot{q}$.

The mass matrix in rectangular coordinate x is defined as:

$$M = diag(m_h, m_h, m_l, m_l, I_l, m_t, m_t, I_t, m_b, m_b, I_b, m_s, m_s, I_s, m_f, m_f, I_f, m_f, m_f, I_f) \quad (4)$$

where m_h, m_l, m_t, m_b, m_s and m_f are masses of hip, each leg, each thigh, upper body, each shank and each foot, respectively. I-components are moments of inertia of corresponding parts. Since the mass of the model is distributed as point masses, the angles in x and the moments of inertia in M could be taken off for simplification.

We denote F as the active external force vector in rectangular coordinates. The constraint function is marked as $\xi(q)$, which is used to maintain foot contact with ground and detect impacts. Note that $\xi(q)$ in different walking phases may be different since the contact conditions change. For example, the constraint function in phase B is:

$$\xi(q) = \begin{bmatrix} \theta_3 - \frac{1}{2}(\theta_1 + \theta_2) \\ x_h + l\sin\theta_1 \\ y_h - l\cos\theta_1 \end{bmatrix} \quad (5)$$

We can obtain the Equation of Motion (EoM) by Lagrange's equation of the first kind:

$$M_q\ddot{q} = F_q + \Phi^T F_f \quad (6)$$

$$\xi(q) = 0 \quad (7)$$

where $\Phi = \frac{\partial \xi}{\partial q}$. M_q is the mass matrix in the generalized coordinates: $M_q = T^T M T$. F_q is the active external force in the generalized coordinates:

$$F_q = T^T F - T^T M \frac{\partial T}{\partial q}\dot{q}\dot{q} \quad (8)$$

Equation (7) can be transformed to the followed formation:

$$\Phi\ddot{q} = -\frac{\partial(\Phi\dot{q})}{\partial q}\dot{q} \quad (9)$$

Then the EoM of matrix formation can be obtained from Equation (6) and Equation (9):

$$\begin{bmatrix} M_q & -\Phi^T \\ \Phi & 0 \end{bmatrix}\begin{bmatrix} \ddot{q} \\ F_f \end{bmatrix} = \begin{bmatrix} F_q \\ -\frac{\partial(\Phi\dot{q})}{\partial q}\dot{q} \end{bmatrix} \quad (10)$$

The equation of strike moment can be obtained by integration of Equation (6):

$$M_q\dot{q}^+ = M_q\dot{q}^- + \Phi^T I_f \quad (11)$$

where $\dot{q}^+$ and $\dot{q}^-$ are the velocities of generalized coordinates after and before the strike, respectively. $I_f = \lim_{t^- \to t^+}\int_{t^-}^{t^+} F_f dt$ is the impulse acted on the walker. Since the strike is modeled as a fully inelastic impact, the walker satisfies the constraint function $\xi(q)$. Thus the motion is constrained by the followed equation after the strike:

$$\frac{\partial \xi}{\partial q}\dot{q}^+ = 0 \quad (12)$$

Then the equation of strike of matrix formation can be obtained from Equation (11) and Equation (12):

$$\begin{bmatrix} M_q & -\Phi^T \\ \Phi & 0 \end{bmatrix}\begin{bmatrix} \dot{q}^+ \\ I_f \end{bmatrix} = \begin{bmatrix} M_q\dot{q}^- \\ 0 \end{bmatrix} \quad (13)$$

III. Typical Walking Gaits

A. Walking sequence

The walking sequence of the flat-foot walker is more complicated than those of the point-foot walkers and the round-foot walkers. When the flat foot strikes the ground, there are two impulses, "heel-strike" and "foot-strike", representing the initial impact of the heel and the following impact as the whole foot contacts the ground. Each foot has three contact cases: foot contact, heel contact and toe contact. Thus there appears several sub-streams in the walking sequence (see Fig. 2), which is different from the cases of point-foot or round-foot models with determined walking sequences. Note that the sequence in Fig. 2 has several sub-stream. One walking step may not include all these phases, moving to which phase at the bifurcation point is based on the contact force. The contact of stance foot is modeled by two ground reaction forces act on the two endpoints of the foot, respectively. If one of the forces decreases below zero in the direction orthogonal to the ground, the corresponding endpoint of the stance foot will lose contact with ground and the stance foot will rotate around the other endpoint. The dynamic switching of the walking phases is more close to real human walking.

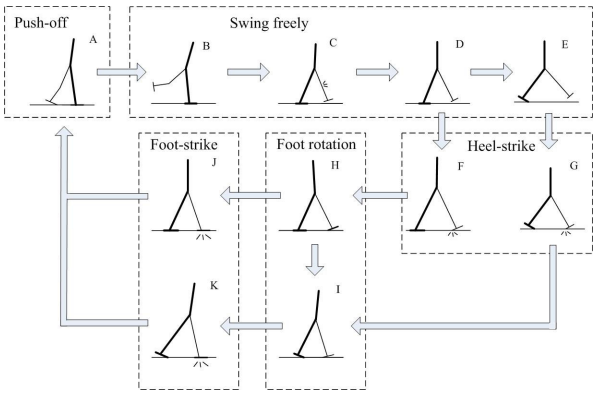

Fig. 2. Walking sequence of the dynamic walker with flat feet and compliant ankle joints.

Then we describe the motion characteristics of each walking phase: Phase A is the push-off phase. The trailing foot rotates around toe with a push-off effect. The foot will lift up when the ground force acted on the toe decreases to zero, which means that the toe loses contact with ground. Then the walker will move to phase B. In phase B, C, D and E, the swing leg of the walker swings freely with no contact with ground. If the heel of trailing foot loses contact with ground before the leading foot strikes ground, the walker will move to phase E, otherwise the walker will move to phase F. Phase F and G are heel-strike phases. The difference between the two phases are the constraint condition of the trailing foot. After heel-strike, the foot of leading leg rotates around heel. In phase H, the whole trailing foot maintains contact with ground. If the contact force act on the heel of rear leg decreases to zero, the model will move to phase I. After foot rotation phases, the walker moves to foot-strike phases, including phase J and K. The difference between the two phases is the constraint of trailing leg. After foot-strike, the stance leg and the swing leg will be swapped and another walking cycle will begin.

Note that Fig. 2 does not include all possible phases. For example, if the contact force act on the toe of trailing leg decreases to zero in phase I, the trailing leg will lose contact with ground, and the model will move to phase B directly after foot-strike, which means that the push-off phase is skipped in this walking step. The walking gaits without push-off are rarely found in real human walking. Thus we ignore these gaits in this paper for their atypical performance.

B. Walking gaits

The walking gaits are classified by the sequence of walking phases in this study. According to the walking sequence discussed above, dynamic bipedal walking with flat feet and compliant joints has three possible gaits (see Fig. 3):

- Gait 1: "$A \rightarrow B \rightarrow C \rightarrow D \rightarrow F \rightarrow H \rightarrow J \rightarrow A$" (see Fig. 3(a)). The whole foot of stance leg keeps contact with ground till foot-strike of swing leg. This gait often has a short step length.
- Gait 2: "$A \rightarrow B \rightarrow C \rightarrow D \rightarrow F \rightarrow H \rightarrow I \rightarrow K \rightarrow A$" (see Fig. 3(b)). The heel of stance leg loses contact with ground before foot-strike of swing leg. This gait is very similar to that of human normal walking.
- Gait 3: "$A \rightarrow B \rightarrow C \rightarrow D \rightarrow E \rightarrow G \rightarrow I \rightarrow K \rightarrow A$" (see Fig. 3(c)). The heel of stance leg loses contact with ground before heel-strike of swing leg. This gait often has a relatively large step length.

These three walking gaits can be characterized by step length. Gait 1 with a short step length is often found in walking in a crowded queue. The step length is confined in a small range since the limited free space. Gait 2 with a moderate step length performs a great resemblance to human normal walking. Gait 3 often appears in the large step length walking for stepping over small obstacles or pits. To illustrate the importance of step length in walking gait selection, we take human walking gaits as references. A person was asked to walk with predeterminate step length on level ground (see Fig. 4). The results show that different step lengths lead to different walking gaits which show a great resemblance to the three dynamic walking gaits in Fig. 3.

C. Actuation mode

We added a piecewise constant hip torque to actuate the walker to travel forward on level ground. The hip torque may be different in different phases. The torque is relatively larger in push-off phase and double-support phase to actuate the swing foot to leave ground and compensate the energy loss at heel-strike, and is near zero in the freely swing phase based on the fact that the muscles of the swing leg are generally silent [9]. Torsional springs are added at ankle joints to represent ankle stiffness. Several researches indicate that ankle walking behavior in humans is quite similar to that of a torsional spring [15]. To improve the performance of walking and achieving various walking gaits, we set different values of ankle stiffness during the stance phase, which

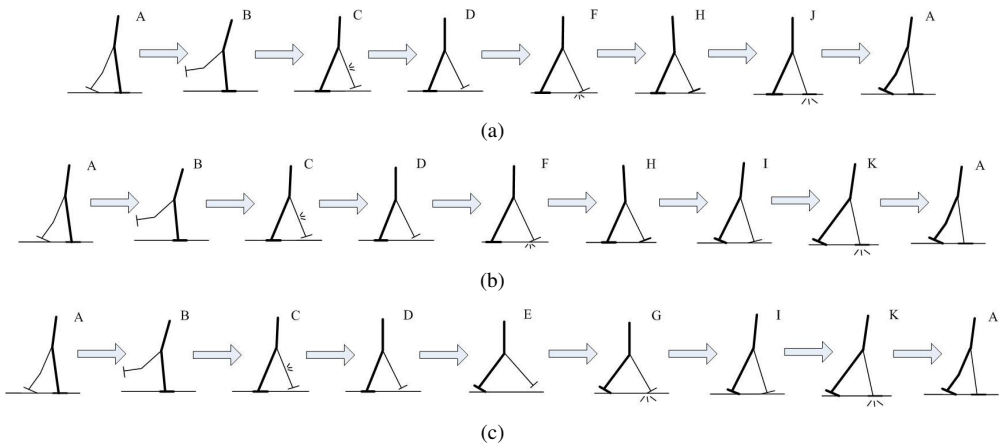

Fig. 3. Three typical dynamic bipedal walking gaits with flat feet and compliant ankle joints.

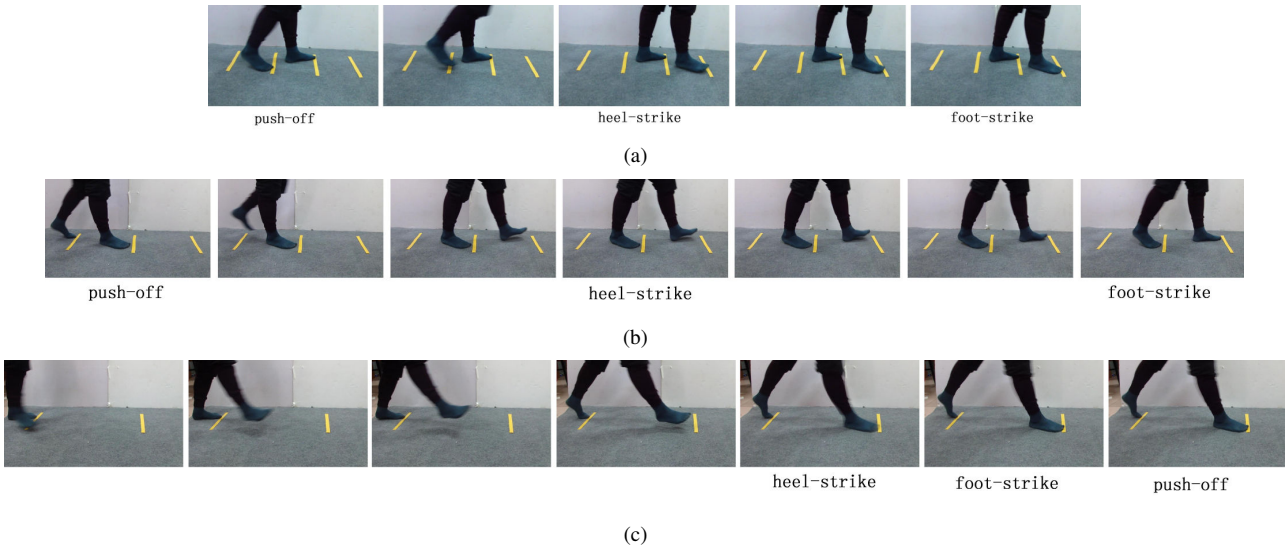

Fig. 4. Snapshots of real human walking. The feet are constrained to contact ground at predefined positions as toes stop at yellow lines. The step length (the distance between contiguous yellow lines): (a) 0.3m; (b) 0.5m; (c) 0.8m. Push-off phase of the second step but not the first step is shown in (c) for the limitation of the angle of view of the camera.

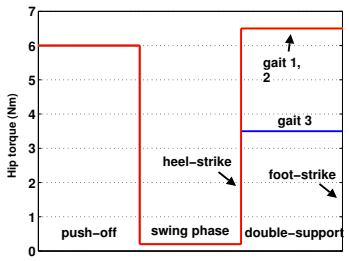

Fig. 5. Actuation pattern for the three gaits. Gait 1 and gait 2 have the same pattern, described by the red line, as the two gaits have a lot of similar characteristics. The hip torque of gait 3 is different only for the double-support phase, illustrated by the blue line.

has a higher resemblance with human normal walking [14]. Similar approach has been used in recent studies [13]. The ankle stiffness has a larger value when the leg has passed the vertical line during foot-flat phase. During the rest of stance the ankle stiffness is lower. The ankle torque changes continuously at the switching of ankle stiffness. The ankle does a amount of net work during one step, which is taken consider into the calculation of energetic efficiency.

In the simulation, stable cyclic walking is searched for various combination of actuation pattern and ankle stiffness. A typical representative of each gait is chosen for comparison, which is illustrated in detail in the next section. The hip torques of the representatives of the three gaits are shown in Fig. 5. The two ankle stiffness values of each gait are: gait1, $30Nm/rad$, $54Nm/rad$; gait2, $50Nm/rad$, $90Nm/rad$; gait3, $35Nm/rad$, $95Nm/rad$. Both the hip actuation mode and the ankle behavior are predefined with no active control during the walking motion.

IV. Results

All simulations and data processing were performed using Matlab 7 (The Mathworks, Inc., Natick, MA). Parameters values used in the analysis are obtained from Table I. All

TABLE I

PARAMETER VALUES IN SIMULATIONS. ALL MASSES AND LENGTHS ARE NORMALIZED BY LEG MASS AND LEG LENGTH, RESPECTIVELY.

Parameter	Value	Parameter	Value
leg mass m_l	0.1538	thigh mass m_t	0.1077
shank mass m_s	0.0461	foot mass m_f	0.0355
body mass m_b	0.355	hip mass m_h	0.2663
leg length l	1	thigh length l_t	0.55
distance from hip to CoM of thigh c_t	0.2750	foot length l_f	0.25
distance from knee to CoM of shank c_s	0.2250	shank length l_s	0.45
distance from ankle to CoM of foot c_f	0.0250	upper body length l_b	0.75
distance from hip to CoM of upper body c_b	0.3750	gravitational acceleration g	$9.8m/s^2$

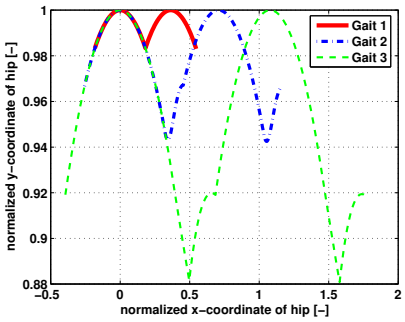

Fig. 6. Hip trajectories of different walking gaits. Both x-coordinate and y-coordinate are normalized by leg length.

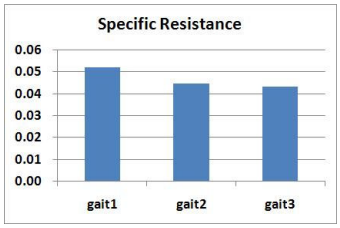

Fig. 8. Specific resistance of different gaits.

mass and length are normalized by total mass and leg length respectively.

A. Walking trajectories of different gaits

In the experiments, we first compared the walking motion under the same mechanical parameters (see Table I) but different initial conditions. Hip tracks in two steps of the three dynamic walking gaits are shown in Fig. 6. One can found the obvious difference of step length by comparison of the trajectories. The leg trajectories of the dynamic walking of Gait 1, Gait 2 and Gait 3 are shown in Fig. 7.

B. Comparison of efficiency and stability of different gaits

Energetic efficiency is an important characteristic to evaluate walking performance. In this paper, walking efficiency is measured by the nondimensional form of 'specific resistance' (energy consumption per kilogram mass per distance traveled per gravity), which is commonly used in the studies of dynamic walking. The energetic efficiency of the walking models with different step length is shown in Fig.8. Dynamic walking with Gait 1 has a specific resistance of 0.0518. It is more efficient than the passive dynamic model with upper

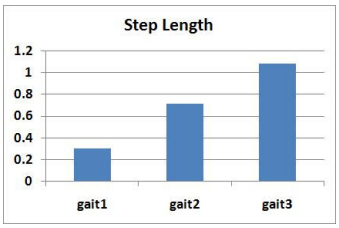

Fig. 10. Step length normalized by leg length of different gaits.

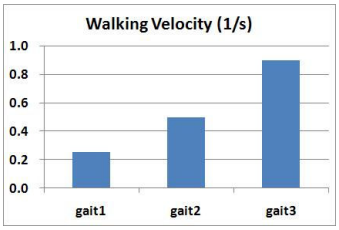

Fig. 11. Walking velocity normalized by leg length of different gaits.

body. The specific resistance of walking with Gait 2 and with Gait 3 are 0.0443 and 0.0432, respectively. Simulation results show that walking in Gait 1 costs much more energy in average.

The stability of the dynamic walking in the three gaits can be analyzed by the approach of limit cycle analysis as mentioned in [6]. We found that walking in Gait 2 performs better in global stability than walking in Gait 1 and in Gait 3, since the allowable errors of Gait 2 are much larger. This can be inspected by the evaluation of the basin of attraction as shown in Fig.9, which is the complete set of initial conditions that eventually result in cyclic walking motion.

C. Relation between step length and walking performance

We have compared motion characteristics of different gaits above. Then we investigate the relation between step length and walking performance. Step length and walking velocity of the three walking gaits are shown in Fig. 10 and Fig. 11, respectively.

The results show that step length reflects walking velocity to a certain extent. The speed of Gait 3 with a large step length is much larger than those of gait 1 and gait 2. Contrarily, walking of gait 1 with the shortest step length is the slowest. Comparison of specific resistance (see Fig. 8) shows Gait 1 consumes much more energy than other gaits. Gait 2 and Gait 3 are more efficient. Thus Gait 3 performs

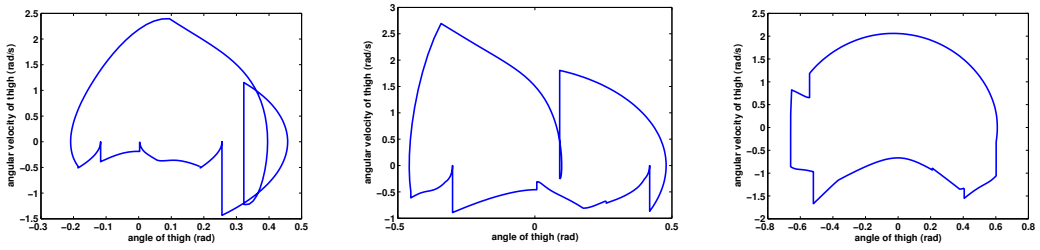

(a) (b) (c)

Fig. 7. Leg trajectories of the dynamic walking with different gaits. (a): the motion cycle of Gait 1 with small step length; (b): the motion cycle of Gait 2 with moderate step length; (c): the motion cycle of Gait 3 with large step length.

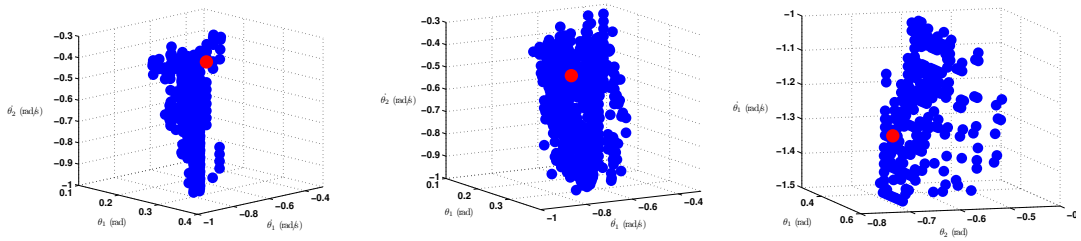

(a) (b) (c)

Fig. 9. Basin of attraction of dynamic walking model of different gaits. (a): Gait 1; (b): Gait 2; (c): Gait 3. The blue points represent region of initial conditions that eventually result in the cyclic walking motion. The cyclic motion is indicated with a red point. Parameters values used in the analysis are obtained from TableI.

well in both velocity and efficiency. However, Gait 3 has poor stability, which can be found by comparison of the basin of attraction of different gaits. The allowable errors of Gait 3 are much smaller than that of gait 2. Consequently, Gait 2 may be the best gait in comprehensive characteristics, while Gait 3 obtains larger velocity by decreasing stability.

V. Conclusion

In this paper, we have presented a dynamic bipedal walking model with compliant joints and flat feet. The bipedal model travels with dynamic series of phases due to complicated contact cases of flat feet. The effects of step length on gait selection was studied in simulations. Experimental results showed that step length plays an important role in gait selection. Comparison of motion characteristics of different gaits indicated that long step length usually results in large velocity. The gait with largest velocity has a relatively poor stability, which means there is partly conflict of velocity and stability. The results show that the walking gait with smallest step length performs worst in efficiency.

There are several ways to extend this work. Other special walking gaits could be added to this research. In addition, the dynamic walking model can be improved by adding certain active control to chose the required gait. Future studies may explain the intrinsic mode of gait selection and gait transition, and guide to realize more practical passivity-based robot prototypes.

References

[1] K. Hirai, M. Hirose, Y. Haikawa, T. Takenaka, The development of the Honda Humanoid robot, *Proc. of the IEEE International Conference on Robotics and Automation*, 1998, pp. 1321-1326.

[2] M. Vukobratovic, A. Frank, D. Juricic, On the Stability of Biped Locomotion, *IEEE Transactions on Biomedical Engineering*, vol. 17, no. 1, 1970.

[3] T. McGeer, Passive dynamic walking, *International Journal of Robotics Research*, vol. 9, pp. 68-82, 1990.

[4] M. Garcia, A. Chatterjee, A. Ruina, M. Coleman, The simplest walking model: stability, complexity, and scaling, *ASME Journal of Biomechanical Engineering*, vol. 120, pp. 281-288, 1998.

[5] A. D. Kuo, Energetics of actively powered locomotion using the simplest walking model, *ASME Journal of Biomechanical Engineering*, vol. 124, pp. 113-120, 2002.

[6] M. Wisse, A. L. Schwab, F. C. T. Van der Helm, Passive dynamic walking model with upper body, *Robotica*, vol. 22, pp. 681-688, 2004.

[7] S. Mochon, T. A. McMahon, Ballistic walking, *Journal of Biomechanics*, vol. 13, no. 1, pp. 49-57, 1980.

[8] A. Ruina, J. E. A. Bertram, M. Srinivasan, A collisional model of the energetic cost of support work qualitatively explains leg sequencing in walking and galloping, pseudo-elastic leg behavior in running and the walk-to-run transition, *Journal of Theoretical Biology*, vol. 237, no. 2, pp. 170-192, 2005.

[9] M. Kwan, M. Hubbard, Optimal foot shape for a passive dynamic biped, *Journal of Theoretical Biology*, vol. 248, pp. 331-339, 2007.

[10] Q. Wang, Y. Huang, L. Wang, Passive dynamic walking with flat feet and ankle compliance, *Robotica*, vol. 28, no. 3, pp. 413-425, 2010.

[11] M. Wisse, D. G. E. Hobbelen, R. J. J. Rotteveel, S. O. Anderson, G. J. Zeglin, Ankle springs instead of arc-shaped feet for passive dynamic walkers, *Proc. of the 2006 IEEE International Conference on Humanoids*, 2006, pp. 110-116.

[12] D. G. E. Hobbelen, M. Wisse, Ankle joints and flat feet in dynamic walking, *International conference on Climbing and Walking Robots*, 2004.

[13] D. G. E. Hobbelen, M. Wisse, Ankle Actuation for Limit Cycle Walkers, *International Journal of Robotics Research*, vol. 27, no. 6, pp. 709-735, 2008.

[14] I. W. Hunter, R. E. Kearney, Dynamics of human ankle stiffness: variation with mean ankle torque, *Journal of Biomechanics*, vol. 15, no. 10, pp. 747-752, 1982.

[15] C. Frigo, P. Crenna, L. M. Jensen, MomentCangle relationship at lower limb joints during human walking at different velocities, *Journal of Electromyography and Kinesiology*, vol. 6, no. 3, pp. 177-190, 1996.